A&A 511, L5 (2010)
DOI: 10.1051/0004-6361/200913983

Astronomy & Astrophysics

Letter to the Editor

The diffuse radio filament in the merging system ZwCl 2341.1+0000

G. Giovannini[1,2], A. Bonafede[1,2], L. Feretti[2], F. Govoni[3], and M. Murgia[3]

[1] Dipartimento di Astronomia, via Ranzani 1, 40127 Bologna, Italy
[2] Istituto di Radioastronomia – INAF, via P.Gobetti 101, 40129 Bologna, Italy
e-mail: ggiovann@ira.inaf.it
[3] Osservatorio Astronomico di Cagliari – INAF, Strada 54, Loc. Poggio dei Pini, 09012 Capoterra (Ca), Italy

Received 29 December 2009 / Accepted 25 January 2010

ABSTRACT

Context. In some clusters of galaxies, a diffuse non-thermal emission is present, not obviously associated with any individual galaxy. These sources have been identified as relics, mini-halos, and halos according to their properties and position with respect to the cluster center. In a few cases diffuse radio emission has been reported that cannot be identified with a cluster, but with a large scale filamentary region.
Aims. We observe and analyze the diffuse radio emission present in the complex merging structure of galaxies ZwCl 2341.1+0000.
Methods. We obtained VLA observations at 1.4 GHz to derive a deep radio image of the diffuse emission.
Results. Low resolution VLA images detect diffuse radio emission associated with the complex merging region of size =2.2 Mpc at most. In addition to the previously reported peripheral radio emission, classified as a double relic, diffuse emission is detected along the optical filament of galaxies.
Conclusions. The giant radio source discussed here shows that magnetic fields and relativistic particles are also present in filamentary structures. Possible alternate scenarios are: a giant radio halo in-between two symmetric relics, or the merging of two clusters both hosting a central radio halo.

Key words. magnetic fields – large-scale structure of the Universe – radio continuum: general

1. Introduction

Diffuse non-thermal radio sources with steep spectra have been found in a relatively large number of clusters of galaxies (see e.g., Giovannini et al. 2009 and references therein). These sources are not directly associated with the activity of individual galaxies and are related to physical properties of the whole cluster. According to their properties and location they are commonly classified as relics and halos.

Relics have been found at the cluster peripheries and the most common interpretation is that they are related to shocks that originated from cluster mergers. Halos are located in the central cluster regions and have always been found in clusters with evidence of merger activity, which plays an important role in particle reacceleration in providing the energy that powers these sources (Brunetti et al. 2009; Feretti & Giovannini 2008).

In addition, evidence of non-thermal emission has been found on even larger scales. Bridges of radio emission have been observed in the regions between relics and halos in a few clusters, including Coma (Kim et al. 1989; Giovannini et al. 1990), A2255 (Feretti et al. 1997), and A2744 (Govoni et al. 2001). Diffuse emission has been found at large distances from A2255 (Pizzo et al. 2008) and A2256 (van Weeren et al. 2009a).

Compelling evidence of radio emission from a filament structure was reported by Bagchi et al. (2002), which was identified with the multi-Mpc scale filamentary network of galaxies in the ZwCl 2341.1+0000 region at $z = 0.27$. The authors discuss large-scale shocks that originate in the accretion flows of intergalactic gas, which were detected in the Mpc scale diffuse radio emission. van Weeren et al. (2009b) presented GMRT observations at 610 MHz, 241 MHz, and 157 MHz of this region, in combination with X-ray and optical data. The radio images show two diffuse sources to the north and south of the cluster position, which they classified as double radio relics. These relics are perpendicular to the X-ray axis, which can be considered to be the merger axis. They are assumed to be caused by outward travelling shocks caused by a major merger event. The distance between the two relics is ~2.2 Mpc.

We present new low-resolution VLA images of the diffuse radio emission at 1.4 GHz. Despite the higher frequency of these data, the higher sensitivity to surface brightness allowed us to detect very extended diffuse radio emission, which extends along the optical filament. We discuss its nature and properties.

The intrinsic parameters quoted in this paper are computed for a ΛCDM cosmology with $H_0 = 71$ km s^{-1} Mpc^{-1}, $\Omega_{\rm m} = 0.27$, and $\Omega_\Lambda = 0.73$. At $z = 0.27$, the angular conversion factor is 4.1 kpc/″.

2. Radio images

The ZwCl 2341.1+0000 region was observed for 6 h with the VLA at 1.4 GHz in the D configuration on July 24 2008, at two different pointings, RA = 23h43m40s Dec = +00°20′00″, and RA = 23h43m50s Dec = +00°14′00″, to avoid high primary beam attenuation and bandwidth smearing. Each field was observed for 3 h, and we moved the pointing center every half an hour to achieve wider uv-coverage. Calibration and imaging were performed with the NRAO Astronomical Image Processing System (AIPS). The sources 3C 48, 3C 138, and 2316+040 were used as a primary flux-density calibrator, an absolute reference

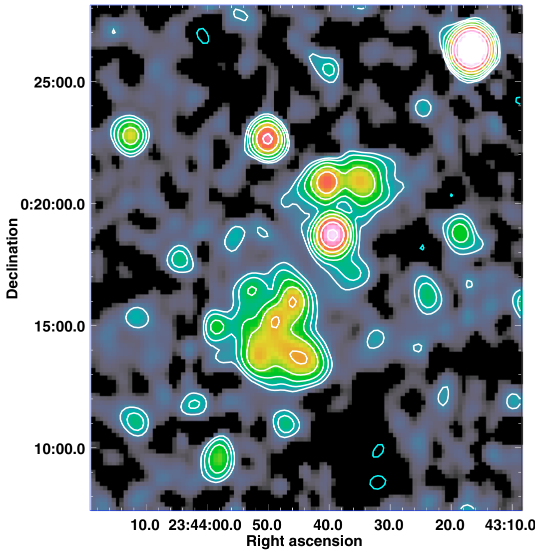

Fig. 1. Radio emission from ZwCl 2341.1+0000 at 1.4 GHz observed at full resolution. The *HPBW* is 50″ × 43″. The first contour is drawn at 3σ level (0.12 mJy/beam), other contours are spaced by a factor 2. The first negative contour (at 3σ level) is in cyan.

for the electric vector polarization angle, and a phase calibrator, respectively. Several cycles of self-calibration were applied to remove residual phase and gain variations. Images of the total intensity (Stokes I) as well as of the Stokes parameters U and Q were produced for the two pointings separately following the common procedures of Fourier-transform, clean, and restore. The images resulting from the two pointings were finally combined using the AIPS task LTESS. We then derived images of both the polarized intensity $P = \sqrt{(U^2 + Q^2)}$ corrected for the positive bias and the polarization angle $\Psi = 0.5 \arctan(U/Q)$. Calibration errors are of the order of 5%.

2.1. Total intensity radio emission

In Fig. 1, we show the final image obtained with natural weights. The diffuse emission is easily visible even if a large number of discrete sources are present. To obtain the image of the diffuse source and measure its flux, we subtracted unrelated discrete sources in the uv plane. After cutting baselines shorter than $2K\lambda$ we produced high resolution images with uniform weight (ROBUST = −5), In these images, only discrete sources are present, whereas the extended diffuse emission is not present being resolved out (see Fig. 2, left panel).

Discrete sources present in our images are related to the list of unrelated sources found by van Weeren et al. (2009b) using GMRT data at lower frequencies, but at higher resolution. A comparison between GMRT flux densities at 610 MHz and at 1.4 GHz, taking into account the different angular resolution and uv-coverage, infers spectral indices in the range 0.8−1.5, expected from extra galactic radio sources (for the strongest subtracted source (A) $\alpha_{0.6}^{1.4} = 1.2$). Clean components were subtracted from the uv data. Using new data sets, we produced low resolution images to enhance the low brightness extended emission. Final images were combined and corrected for the primary beam attenuation. The final combined, primary-beam-corrected image is shown in the right panel of Fig. 2. In this image, the radio emission is continuous and the gap between the northern and southern regions visible in Fig. 1 is no longer present, clearly because of a positive noise in this area, which is enhanced by the slightly larger beam.

2.2. Polarized emission

We investigated the presence of polarized emission in the radio diffuse emission. We produced Stokes Q and U low resolution images. The discrete sources were subtracted as described above for the total intensity image. We derived the polarization angle image and the polarization intensity image without imposing any cut on the uv-range. From the polarization intensity image, we derived the fractional polarization image and considered as valid pixels whose signal-to-noise ratio was >3. This cut was performed to remove possible spurious polarization. The resulting image is shown in Fig. 3. We infer that polarization is detected in the northern and southern components, as well as in the central region.

3. Results

In the final image obtained after subtracting the discrete sources, extended emission was detected, which is consistent with the result of Bagchi et al. (2002). Owing to the higher sensitivity of our image, the diffuse source is well defined. The radio morphology is elongated, clearly following the distribution of both the optical galaxies and the X-ray emission, shown by van Weeren et al. (2009b). We note that the regions of highest brightness are coincident with the two relics presented by van Weeren et al. (2009b). In the central region, we detect low surface brightness emission at the level of 0.4–0.6 mJy/beam (corresponding to $\sim 7 \times 10^{-5}$ mJy/arcsec^2), which could be detected at 610 MHz with a 15″ beam only if the spectral index $\alpha_{0.6}^{1.4}$ is steeper than 2.5−3.

The total size of the diffuse emission is ~2.2 Mpc. The measured total flux at 1.4 Ghz is 28.5 mJy, corresponding to a radio power $\log P_{1.4} = 23.66$ W/Hz. The radio emission is irregular and decreases from the two bright outer regions toward the cluster center. A plateau of radio emission, at the level of about 0.6 mJy/beam, is present at the location of the southernmost X-ray peak, detected by Chandra and published in Fig. 1 of van Weeren et al. (2009b).

We detect polarized emission from large areas of the diffuse radio source, both from the outer and the central regions. The polarized flux is more prominent in the eastern side of the extended source. Once the discrete sources have been subtracted, the total polarized flux is ~2.4 mJy. The polarized percentage in both the northern and the southern bright regions is ~15% and 8%, respectively, while the mean fractional polarization in the central region is ~11%. The polarization vectors are very regular and oriented toward the NE–SW direction in the northern source region. In the other regions, they follow the eastern edge of the total intensity emission still showing some level of ordering.

From present images and following the detailed discussions of Bagchi et al. (2002), and van Weeren et al. (2009b), we ruled out the identification of this extended emission as a giant radio galaxy, and we instead compared its properties with those of radio halos presented in Giovannini et al. (2009). The 2.2 Mpc size is remarkably high but comparable to that of the radio halos in A2163 and 1E0657-56. In contrast, the total radio power at 1.4 GHz is considerably lower than the expected value for a giant radio halo from the correlation between halo's size and radio power shown in Giovannini et al. (2009, and references therein).

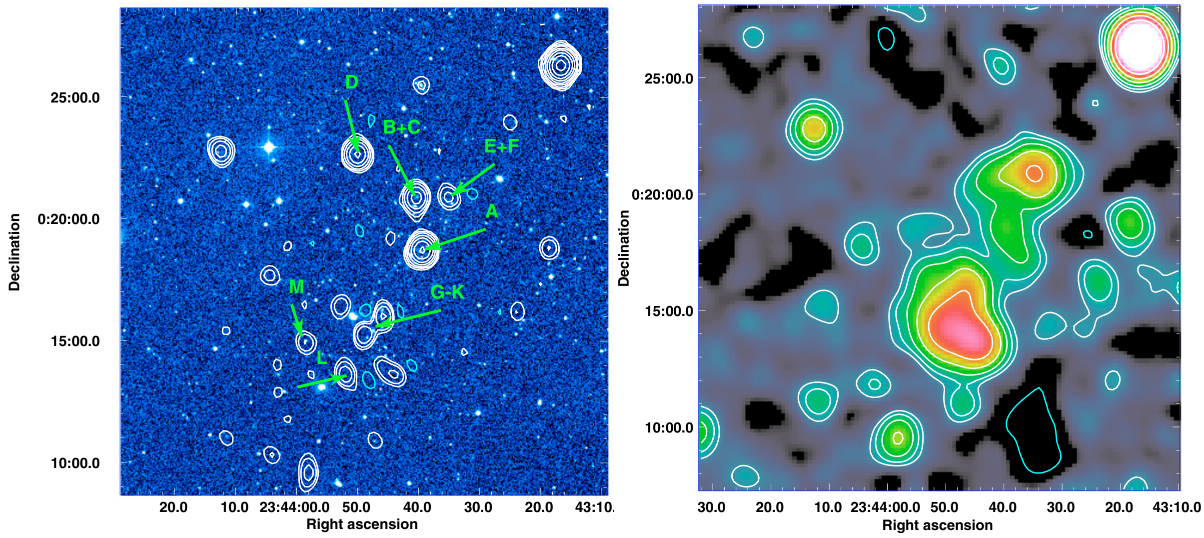

Fig. 2. *Left*: the large-scale galaxy distribution around ZwCl 2341.1+0000 is shown in colors. The optical image is from GSCII (Lasker et al. 2008). Contours of the radio emission from discrete sources (see text) are overlaid. The *HPBW* is 39″ × 35″. The first contour is drawn at 3σ level (0.15 mJy/beam). Following contours are spaced by a factor of 2. The first negative contour at 3σ level is displayed in cyan. Labels refer to the sources found by van Weeren et al. (2009b). *Right:* colors and contours refer to the radio emission after the subtraction of the discrete sources. The *HPBW* is 83″×75″. The first contour is drawn at 3σ level (0.15 mJy/beam). Following contours are spaced by a factor of 2.

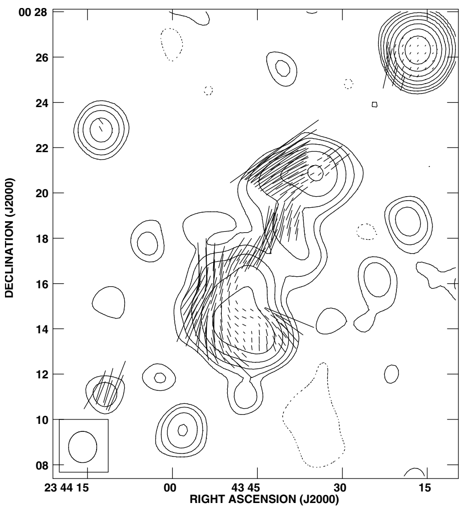

Fig. 3. Polarized emission from ZwCl 2341.1+0000 at 1.4 GHz. Contours show the total-intensity emission at low resolution (see Fig. 2). Lines refer to the E vectors. Their orientations represent the projected E-field uncorrected for the Galactic rotation. Their length is proportional to the fractional polarization: 1″ corresponds to 0.2%.

4. Discussion

Owing to the high sensitivity to surface brightness of our present observations we have detected radio emission of very low brighthness in the ZwCl 2341.1+0000 complex. The data reported in this paper detect diffuse radio emission along the whole optical filament, as first reported by Bagchi et al. (2002), in addition to the bright radio regions located at the outer source boundary, where van Weeren et al. (2009b) suggested the existence of two relics. The low angular resolution of the present data does not allow us to distinguish between the radio emission of these features and the remaining diffuse emission.

As suggested by Bagchi et al. (2002), the most obvious interpretation is that this region is experiencing a large-scale structure formation, where cosmic shocks originating in a complex multiple merger are able to accelerate particles and amplify seed magnetic fields. The large-scale radio emission would originate in large-scale shocks and possibly turbulence, and the identification of single radio-source components such as relics, would be problematic. The existence of significant polarized emission image can be easily explained in this scenario. The shocks connected to large-scale filaments are indeed expected to compress the magnetic field, allowing the detection of polarized emission also at this low resolution. Furthermore, we note that the lower gas density of filaments relative to clusters would cause a smaller amount of depolarization and internal Faraday rotation, which could explain the ordered features revealed by the polarization image. The high fractional polarization in the eastern side could be related to the direction and dynamics of the merging process.

An alternate possibility could be that the extended emission in this cluster consists of two peripheral relics and a central radio halo, as in the clusters A1758 (Giovannini et al. 2009) and RXCJ1314.4-2515 (Feretti et al. 2005; Venturi et al. 2007). In this scenario, shocks originating in the merging processes of this complex structure could produce the peripheral relics, while large-scale turbulence at the cluster center enhanced by X-ray data (van Weeren et al. 2009b) could produce the central halo. Although it is difficult in ZwCl 12341.1+0000 to distinguish between the relic and halo emission, we estimate that the radio halo size is ~4′ (~1 Mpc) with a flux density ~10 mJy (log $P_{1.4}$ 23.2 W/Hz), and that the northern and southern relics have flux densities of ~5 mJy and 13 mJy, respectively. The spectral index of the two relics between 1.4 GHz and 610 MHz, estimated from the present data and those by van Weeren et al. (2009b), is ~1.2 (for both relics). This value is higher with respect to $\alpha_{241}^{610} = 0.49$ and 0.76 for the N and S relics, respectively, reported by van Weeren et al. (2009b). Although this may be due to a genuine flattening at low frequency, we note that because of different UV coverages and sensitivities, it is not possible to derive firm conclusions about the spectral index properties.

From the image presented in this paper, we have found that the central radio halo is likely to show a quite irregular structure, although its radio size and power are in good agreement with the correlation between radio power and size reported by Giovannini et al. (2009). The two possible relics are also peculiar, indeed their shape is neither regular nor elongated as in typical relics such as 1253+275 in the Coma cluster (Giovannini et al. 1991) or the double relics in A3376 (Bagchi et al. 2005), and A3667 (Röttgering et al. 1997). However, exceptions are known in the literature such as the relics in A1664 (Govoni et al. 2001) and A548b (Feretti et al. 2006). The presence of polarized emission in the two relics favor this scenario, whereas the detection of polarization in the central halo does not. Radio halos are indeed, typically unpolarized with upper limits of a few percent. The only two cases known in which polarized emission has been detected from radio halos are the cluster Abell 2255 (Govoni et al. 2005) and MACS J0717+3745 (Bonafede et al. 2009).

As a third possiblity, we recall the two halos detected for the first time in the double cluster system A399/A401 (Murgia et al. 2010). These two clusters are probably in a pre-merging phase: the X-ray excess, the slight temperature increase in the region between the two clusters, and the relatively high metallicity of the hot IGM in the same region are evidence of a physical link between this pair of clusters (Murgia et al. 2010, and references there in). In this scenario, we may interpret the complex radio emission in ZwCl 2341.1+0000 as an evolved case of two clusters, both hosting a radio halo. During the ongoing merger process, the two radio halos would appear as brighter diffusely radio-emitting regions, connected by a faint radio bridge, which could orginate from the cluster interaction as in the bridge in the Coma cluster (Kim et al. 1989). After the merger, the two clusters would eventually create a giant radio halo. A major concern about this scenario is that from the optical isodensity contours presented by van Weeren et al. (2009b), in the brightest radio-emitting regions there is no evidence of a galaxy overdensity, which is the expected signature of the two merging clusters. Furthermore, the detected polarization flux could not obviously be reconciled with this scenario.

5. Conclusions

Diffuse radio emission identified with the ZwCl 2341.1+0000 complex has been detected along the whole filament of galaxies, in agreement with the results of Bagchi et al. (2002). We confirm that the regions of highest radio brightness are located at the outer source boundary, where van Weeren et al. (2009b) suggested that two relics exist. The angular resolution of the present data does not allow us to separate the radio emission of the various features. We suggest three possible scenarios:

1. The cluster is the site of cosmic shocks originating in multiple mergers during the large-scale structure formation, as proposed by Bagchi et al. (2002). In this case, the radio emission would be related to the galaxy filament as a whole. The polarized emission image could easily be reconciled with this scenario, as the shocks connected to large-scale filaments are expected to compress the magnetic field to a high degree of ordering.
2. The diffuse radio emission could consist of a central radio halo and two opposite radio relics, as found in A1758 or RXCJ1314.4-2515. Despite the irregular structure of the central halo, its size and power would be consistent with the correlation between radio power and size reported by Giovannini et al. (2009). The structures of the two relics is different from those of typical elongated relics, although some other irregular relics have been (A1664, A548b). The fractional polarization detected in the diffuse source is consistent with the polarization of relics, whereas the radio halos are generally unpolarized (but see A2255 and MACS J0717+3745).
3. The complex structure could originate in a double cluster, hosting two radio halos, similar to the cluster system A399/A401 (Murgia et al. 2010), but at a later stage of merging, therefore the system has developed a radio bridge between the two interacting clusters. The presence of polarized flux cannot be easily reconciled with this scenario, as radio halos are generally unpolarized. Moreover, from the optical isodensity contours presented by van Weeren et al. (2009b), in the brightest radio-emitting regions there is no evidence of a galaxy overdensity, which is the expected signature of the two merging clusters.

Acknowledgements. The National Radio Astronomy Observatory is operated by Associated Universities, Inc., under cooperative agreement with the National Science Foundation.

References

Bacchi, M., Feretti, L., Giovannini, G., & Govoni, F. 2003, A&A, 400, 465
Bagchi, J., Enßlin, T. A., Miniati, F., et al. 2002, New Astron., 7, 249
Bagchi, J., Durret, F., Lima Neto, G. B., et al. 2005, Proc. 29th Int. Cosmic Ray Conference., Pune, India, ed. B. Sripathi Acharya, et al., Tata Inst. of Fundamental Research, 3, 241
Bonafede, A., Feretti, L., Giovannini, G., et al. 2009, A&A, 503, 707
Brunetti, G., Cassano, R., Dolag, K., & Setti, G. 2009, A&A, 507, 661
Feretti, L., Boehringer, H., Giovannini, G., & Neumann, D. 1997, A&A, 317 432
Feretti, L., Schuecker, P., Böhringer, H., et al. 2005, A&A, 444, 157
Feretti, L., Bacchi, M., Slee, O. B., et al. 2006, MNRAS, 368, 544
Feretti, L., & Giovannini, G. 2008, A Pan-Chromatic View of Clusters of Galaxies and the Large-Scale structure, ed. M. Plionis, O. Lopez-Cruz, & D. Hughes, Lecture Notes in Physics, 740.474, 143
Giovannini, G., Kim, K. T., Kronberg, P. P., & Venturi, T. 1990, Proceedings of the 140th, ed. R. Beck, P. P. Kronberg, & R. Wielebinski (Kluwer Academic Publishers), IAU Symp., 492
Giovannini, G., Feretti, L., & Stanghellini, C. 1991, A&A, 252, 528
Giovannini, G., Bonafede, A., Feretti, L., et al. 2009, A&A, 507, 1257
Govoni, F., Feretti, L., Giovannini, G., et al. 2001, A&A, 376, 803
Govoni, F., Murgia, M., Feretti, L., et al. 2005, A&A, 430, L5
Kim, K.-T., Kronberg, P. P., Giovannini, G., & Venturi, T. 1989, Nature, 341, 720
Lasker, B. M., Lattanzi, M. G., McLean, B. J., et al. 2008, AJ, 136, 735
Murgia, M., Govoni, F., Feretti, L., & Giovannini, G. 2010, A&A, 509, 86
Pizzo, R. F., de Bruyn, A. G., Feretti, L., & Govoni, F. 2008, A&A, 481, L91
Röttgering, H. J. A., Wieringa, M. H., Hunstead, R. W., et al. 1997, MNRAS, 290 577
van Weeren, R. J., Intema, H. T., Oonk, J. B. R., et al. 2009a, A&A, 508, 1269
van Weeren, R. J., Röttgering, H. J. A., Bagchi, J., et al. 2009b, A&A, 506, 1083
Venturi, T., Giacintucci, S., Brunetti, G., et al. 2007, A&A, 463, 937